Analyst

PAPER

Partial filling affinity capillary electrophoresis including adsorption energy distribution calculations – towards reliable and feasible biomolecular interaction studies†

Joanna Witos,[a] Jörgen Samuelsson,[b] Geraldine Cilpa-Karhu,[a] Jari Metso,[c] Matti Jauhiainen[c] and Marja-Liisa Riekkola*[a]

In this work, a method to study and analyze the interaction data in free solution by exploiting partial filling affinity capillary electrophoresis (PF-ACE) followed by adsorption energy distribution calculations (AED) prior model fit to adsorption isotherms will be demonstrated. PF-ACE-AED approach allowed the possibility to distinguish weak and strong interactions of the binding processes between the most common apolipoprotein E protein isoforms (apoE2, apoE3, apoE4) of high density lipoprotein (HDL) and apoE-containing HDL$_2$ with major glycosaminoglycan (GAG) chain of proteoglycans (PGs), chondroitin-6-sulfate (C6S). The AED analysis clearly revealed the heterogeneity of the binding processes. The major difference was that they were heterogeneous with two different adsorption sites for apoE2 and apoE4 isoforms, whereas interestingly for apoE3 and apoE-containing HDL$_2$, the binding was homogeneous (one site) adsorption process. Moreover, our results allowed the evaluation of differences in the binding process strengths giving the following order with C6S: apoE-containing HDL$_2$ > apoE2 > apoE4 > apoE3. In addition, the affinity constant values determined could be compared with those obtained in our previous studies for the interactions between apoE isoforms and another important GAG chain of PGs – dermatan sulfate (DS). The success of the combination of AED calculations prior to non-linear adsorption isotherm model fit with PF-ACE when the concentration range was extended, confirmed the power of the system in the clarification of the heterogeneity of biological processes studied.

Introduction

Novel instrumental analytical techniques and new methods of research are needed to understand biomolecular interactions that occur in extracellular matrix (ECM) and indicate their relationships to atherosclerosis and age-related diseases, most notably Alzheimer disease.

Among lipoprotein particles, HDL and low density lipoproteins (LDL) are the major cholesterol transport vehicles in human circulation.[1] They consist of a hydrophobic core containing mainly cholesteryl esters, triglycerides, fatty acids and fat-soluble vitamins,[2] whereas the surrounding hydrophilic layer is composed of apolipoproteins, a monolayer of phospholipids and unesterified cholesterol. LDL particles display important physiological role of providing some tissues with cholesterol for steroid hormone synthesis while HDL particles function as the key cholesterol carriers back to liver in the process called reverse cholesterol transport.[3,4] Human plasma lipoproteins are involved in the specific interactions with PGs, which are a structural component of ECM of the arterial wall, resulting in the development of atherosclerosis.[5–7] As well known, PGs consist of GAGs, which are unbranched carbohydrate polymers composed of repeating disaccharide units. GAGs, mainly C6S, heparin and DS interact specifically with proteins of LDL and HDL such as apolipoprotein B-100 (apoB-100) and apoE affecting their functions.[8] Both apoE and apoB-100 have similar positively charged amino acids regions that mediate their binding to GAGs, and especially the retention of apoE-containing HDL particles indicate atherogenic processes.[9,10]

[a]Laboratory of Analytical Chemistry, Department of Chemistry, P.O. Box 55, FIN-00014 University of Helsinki, Finland. E-mail: marja-liisa.riekkola@helsinki.fi; Tel: +358-40 5058848
[b]Department of Engineering and Chemical Sciences, INTERACT, Karlstad University, SE-651 88 Karlstad, Sweden
[c]National Institute for Health and Welfare, Public Health Genomics Unit, Biomedicum, FIN-00290 Helsinki, Finland
†Electronic supplementary information (ESI) available. See DOI: 10.1039/c5an00210a

ApoE, an exchangeable apolipoprotein component of very-low density lipoprotein (VLDL) and HDL particles, participates in lipid transport in human plasma and brain.[11,12] The human apoE occurs in several isoforms, of which the most known apoE2, apoE3 and apoE4 differ from each other by the amino acids 112 and 158 affecting their metabolic properties and relation to diseases. ApoE2 (112-Cys; 158-Cys) binds defectively to LDL receptor and is linked to hyperlipoproteinemia type III, while apoE3 (112-Cys; 158-Arg) interacts normally and is associated with balanced lipid metabolism.[12] ApoE4 (112-Arg; 158-Arg) is present in about 25–30% of population and is considered as a major genetic factors in heart and neurodegenerative disease, mainly Alzheimer disease. ApoE4 isoform, inheriting from a parent, occurs in about 40% of people who develop Alzheimer disease. However, several studies available cannot yet explain a detailed process of developing Alzheimer and a contribution of apoE4 to its mechanism.

In our previous studies we have demonstrated that partial filling affinity capillary (PF-ACE) technique forms an excellent platform for the interaction study of lipoproteins, PGs and steroids.[13–16] PF-ACE is characterized by small sample and reagent consumptions, relatively fast analysis time, conduction in a free solution (no need to bind ligand to a surface), useful and comprehensive method to investigate the strong interactions between biological compounds. In our most recent study the comparable results achieved for the adsorption data by quartz crystal microbalance, microscale thermophoresis and PF-ACE confirmed us that PF-ACE can be considered as reliable method for accurate adsorption isotherm determination.[16] It has also been evident that in addition to accurately determined adsorption data, the data processing plays important role for the selection of the correct adsorption isotherm model used in the model fitting. Accordingly we have recently improved the data processing for biosensors and liquid chromatography.[14–19] The process contains three different steps: (i) Scatchard plots are used to roughly reveal the category of the adsorption such as if the adsorption isotherm contains inflection points and some initial information about the adsorption energy heterogeneity. (ii) Adsorption energy distributions (AED) are calculated to determine the degree of heterogeneity in the interaction: *i.e.*, how many different adsorption sites are present, their individual energy and their abundance. (iii) Model fit to raw adsorption data are done using models that fulfills both steps above. The first two steps will reduce the number of possible models considerably.[19,20]

The aim of the present work was to demonstrate that the combined PF-ACE-AED approach could be exploited as a sole technique for the investigation of demanding biomolecular interactions, such as the interactions between C6S and three most common isoforms of apoE of HDL, and apoE-containing HDL$_2$ particles. The results achieved proved that this versatile technique is useful for the elucidation of the heterogeneity of interactions including the determination of affinity constants for each interaction resulting in deeper understanding of their biological processes.

Results and discussion

To investigate the binding process and achieve deeper understanding of interactions between apoE and C6S, adsorption isotherms were determined using PF-ACE. The raw adsorption data was analyzed using AED and Scatchard plots followed by adsorption isotherm model fitting to models fulfilling the AED calculations to get a better estimation of heterogeneity of the adsorption process.

Because it is well recognized that the positively charged biomolecules adsorb very easily onto the negatively charged fused silica capillary surface, this phenomenon was avoided by masking the charges of inner capillary wall with stable P2QVP-*b*-PEO diblock copolymer coating.[21] The dynamic coating was always freshly prepared before the interaction studies. To ensure the success of the coating, the electro-osmotic flow (EOF) mobilities were measured by the Williams and Vigh method,[22] and they were in the range of 1.0×10^{-10} to 7.3×10^{-10} m^2 V^{-1} s^{-1} indicating the minor cationic nature of the capillary resulted in very slow anodic EOF. In addition, the EOF was measured between the runs, and the migration times of the analytes were corrected with the EOF values. Then the coated capillary was ready for the clarification of interactions between C6S and the three different apoE isoforms (apoE2, apoE3 and apoE4) and apoE-containing HDL$_2$. The studies were carried out at 25 °C and pH 7.4 (phosphate buffer of I 20 mM as a BGE solution).

The main criteria for the successful study was that the mobility of partially filled C6S, acting as a dispersed phase, should allow interactions of C6S with isoforms of apoE and apoE-containing HDL$_2$. This requirement was met by selecting the anode for the detector end, and making sure that after the voltage was applied, the negative isoforms of apoE or apoE-containing HDL$_2$ could be reached by C6S. In the slightly cationic diblock-copolymer coating, the migration of the highly negatively charged C6S was faster than that of the negatively charged isoforms of apoE and apoE-containing HDL$_2$, which allowed C6S to pass and interact with them. To achieve proper adsorption data for binding study, a wide range of C6S concentration (0.0 mg mL^{-1} to 1.0 mg mL^{-1}) was needed. As seen in Fig. 1, the peaks describing apoE isoforms, C6S, complexes formed could be recognized on each electropherogram. In addition, some impurities and system peaks were detected. The migration time of the excess of C6S remained constant, while the migration time of formed complexes decreased as the amount of negatively charged C6S increased (Fig. 1). The absolute values of the apoE isoform mobilities decreased in the order: apoE2 > apoE3 > apoE4 following their number of charged amino acid residues. Although the changes for apoE2 isoform and apoE-containing HDL$_2$ were minor, data obtained could be still verified by AED calculations (Fig. 1 and S1†).

From the data presented in Fig. 1 and S1† the raw adsorption isotherm data could be determined for the three isoforms of apoE and apoE-containing HDL$_2$ using eqn (2). The raw adsorption data is presented as symbols in Fig. 2–4 and S2† (top left figure). The minimum mobilities were determined
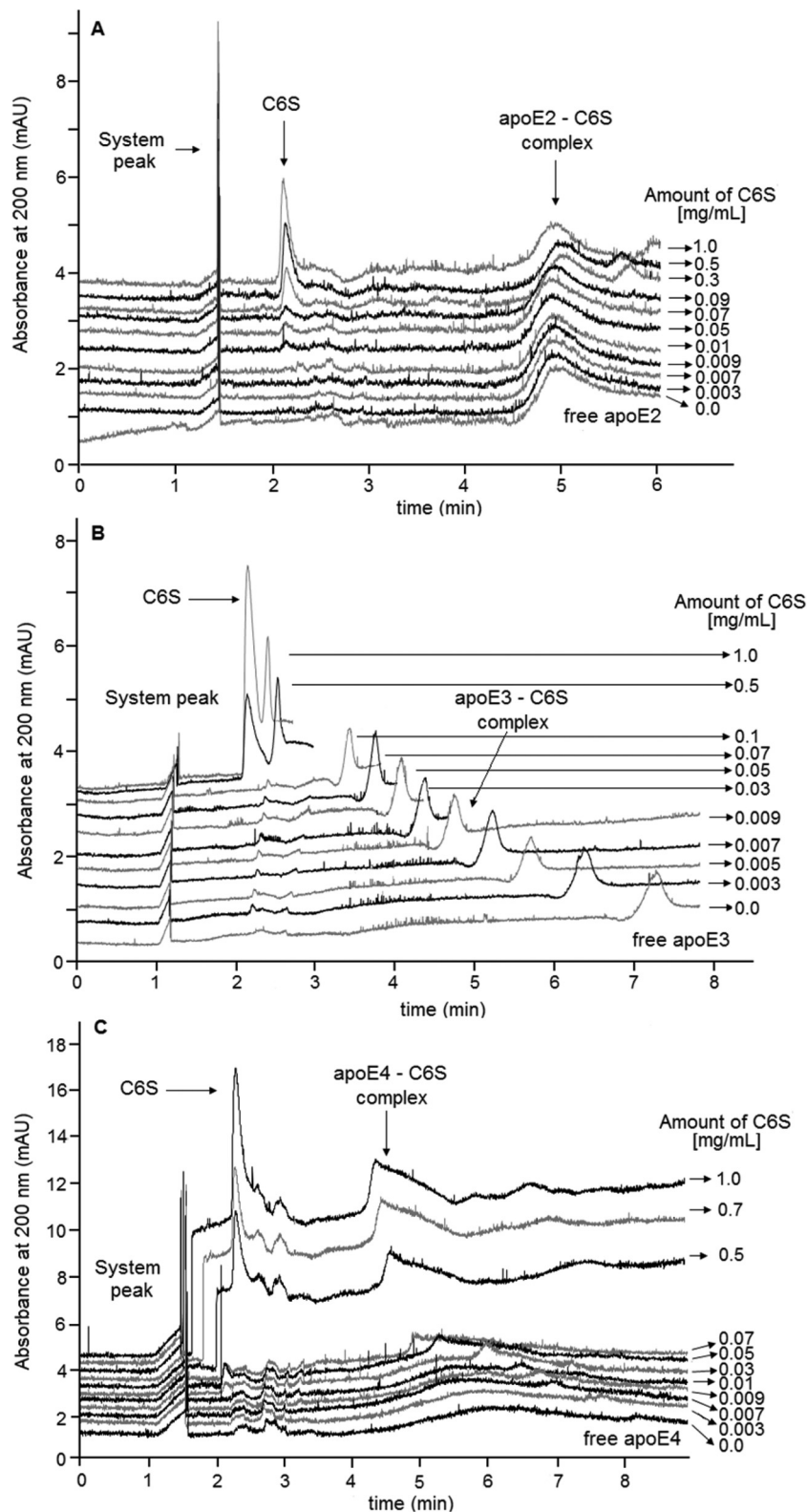
Fig. 1 Electropherograms obtained by affinity capillary electrophoresis with partial filled technique are presented as a function of increased concentration of C6S interacting with (A) apoE2; (B) apoE3; and (C) apoE4. Running conditions: −25 kV, injection time of isoforms of apoE 2 s at 50 mbar, injection time of C6S 3 s at 50 mbar, 25 °C, L_{tot} 38.5 cm, L_{det} 30 cm, UV detection 200 nm, BGE phosphate buffer (pH 7.4, I 20 mM), apolipoprotein concentrations 0.2 mg mL^{-1} for each apolipoprotein, and C6S concentration ranging from 0.000 mg mL^{-1} to 1.0 mg mL^{-1}.
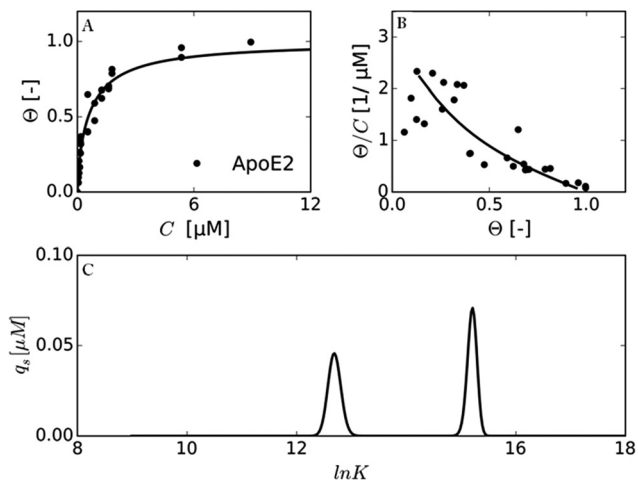
Fig. 2 (A) Adsorption isotherm of apoE2, (B) corresponding Scatchard plot and (C) AED calculations for apoE2–C6S system at 25 °C.
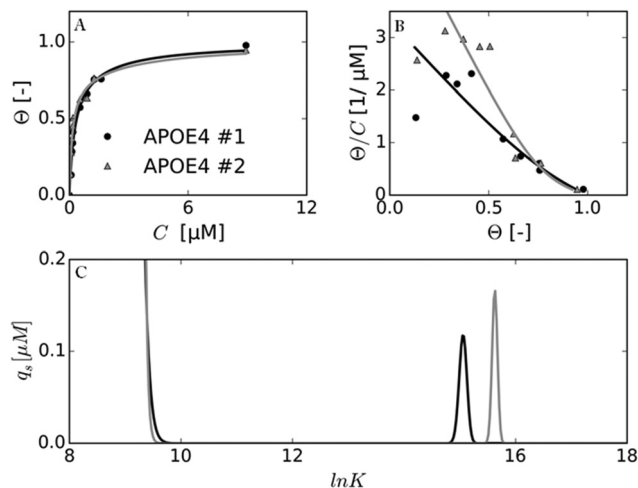

Fig. 4 (A) Adsorption isotherm of apoE4, (B) corresponding Scatchard plot and (C) AED calculations for apoE4–C6S system at 25 °C.
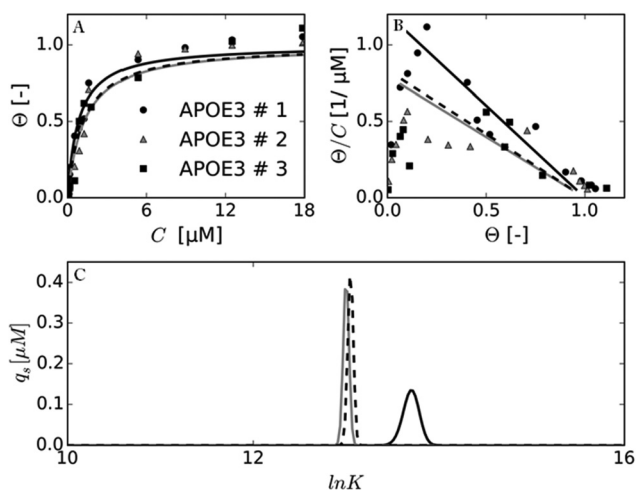

Fig. 3 (A) Adsorption isotherm of apoE3, (B) corresponding Scatchard plot and (C) AED calculations for apoE3–C6S system at 25 °C.

with non-linear fitting at the lowest concentration range while the maximum mobilities were established with linear fitting over the whole concentrations range. From this the affinity constants could be calculated.

For the determination of affinity constants first Scatchard plot analysis was used for getting preliminary insight into the adsorption characteristics (Fig. 2–4 and S2,† top right figure), then AED calculations (Fig. 2–4 and S2,† bottom figure) were exploited to provide insight into the heterogeneity of the adsorption isotherm models before the model fitting, and finally rival adsorption models were fitted to the raw adsorption data by fulfilling previous two steps and classical F-tests were used for the raw adsorption data (Fig. 2–4 and S2,† lines in top figures).

As shown in Fig. 2B, the Scatchard plot of adsorption of apoE2–C6S system is concave indicating that heterogeneous

adsorption models, such as *e.g.* bi-Langmuir, Tóth should be used, because they are adsorption models with heterogeneous adsorption energy distributions with concave Scatchard plots. The Tóth model has unsymmetrical AED while bi-Langmuir equation has two symmetrical AEDs at different adsorption energies (ln K values).[20] The AED presented in Fig. 2C contains two distinct symmetrical distributions that are typical for the bi-Langmuir model: one at lower and another at higher energy with ln K values of around 13 and 15, respectively. The bi-Langmuir model fitted well to the raw adsorption data with R^2 of 0.957. For apoE3–C6S system (Fig. 3), the Scatchard plot is more linear with some scattered data at low concentrations, and by inspecting this data in more detail; we could see that the Scatchard plot became convex. Although convex Scatchard plot could be indication of multilayer adsorption isotherm,[17] in our case more probable reason for this data is experimental noise at the low concentration. However, we could not be certain of using a homogeneous adsorption model, but because the AED contained only one adsorption site, it was obvious that a single site adsorption model should be used. By combining the information obtained from the Scatchard plot, and by assuming that scattered data is due to experimental noise, the AED proved that Langmuir model was a good choice and fitted well to the adsorption data with an average R^2 of 0.959. As seen from Fig. 4B, the Scatchard plot of adsorption of apoE4–C6S system is very scattered and hard to visually determine if it is linear or not. To get more out of the data, the AED were calculated resulting in at least two adsorption sites: unconverted low energy site and converted high energy site with ln K value of around 15. This is quite common situation in adsorption studies and the reason for unconverted low energy site is most probably caused by that too low maximum concentration of apoE4 (due to solubility limitations) were used in the adsorption isotherm acquisition.[17,18,23] The AED proved that a adsorption isotherm with an bimodal AED should be used. The bi-Langmuir model fitted well to the raw

Table 1 Affinity constants (log K_a) for the interactions between GAGs chains of PGs and isoforms of apoE and apoE-containing HDL$_2$

	ApoE2	ApoE3	ApoE4	apoE-containing HDL$_2$
C6S	(I) 6.9 (II) 6.0	(I) 6.0	(I) 6.8 (II) 5.7	(I) 7.3
DS	(I) 6.1	(I) 5.9 (II) 4.8	—	—

adsorption data with an average R^2 of 0.973. Finally, for the adsorption of apoE-containing HDL$_2$-C6S system (Fig. S2†), the scattered Scatchard plot could not again prove if the data is linear or non-linear, and AED calculations were needed to show it to be symmetrical monomodal. This indicates that the Langmuir model was a model of choice and it fitted well to the raw adsorption data with an average R^2 of 0.870.

In Table 1, the association equilibrium constants from the adsorption isotherm model fit is presented. The results enabled the evaluation of the binding strength with C6S giving the following order: apoE-containing HDL$_2$ > apoE2 > apoE4 > apoE3. Seemingly apoE-containing HDL$_2$ indicated the strongest interaction while apoE3 the weakest. One limiting factor here when interpreting our results is that we do not know the isoform(s) in HDL$_2$ preparation. On the other hand, the binding strength may be modulated by other HDL particle surface components located near apoE. One reason for the following order could be differences in the structural composition of apoE isoforms. Clearly the tertiary structure of the apoE-isoforms is an important criteria to the assessment of the interaction strength. ApoE has two domains separated by hinge region, N- and C-terminal. The N-terminal domain (amino acids 1–191) includes the receptor binding region (amino acids 134–150; Arg-172) and forms a four-helix antiparallel bundle, while the C-terminal (amino acids 225–299) contains the major lipid (especially phospholipid) binding region (amino acids 244–272).[24,25] There are differences in a few amino acids among apoE isoforms. ApoE3 has cysteine in the 112th amino acid and arginine in the 158th, whereas apoE2 has cysteines at both sites, and apoE4 has arginines. Essential role of cysteine is a stabilization of the secondary and tertiary protein structures by forming disulfide-linked heterodimer. On the other hand, the presence of arginine enhances the interactions with negatively charged groups in the GAGs. The introduction of one arginine or cysteine group to apoE structure may enhance or abolish the interactions with C6S by changing the accessibility to available adsorption sites.

Another remark is the structural properties of apoE4. ApoE4 has a domain interaction promoted by the arginine in position 112 and by the salt-bridge formation between Arg61-Glu255 maintaining its tertiary structure. However, apoE4 is quite unstable to unfolding, so changes in temperature may affect its structure and makes it unstable taking another globular form. Conversely, apoE3 and apoE2 tend to be less

unstable, have less or no domain interactions and thus have more open structures. The domain interaction contributes to the close proximity of the N- and C-terminals which contain the GAG binding sites and thus may promote higher interactions. This may explain the higher interaction strength of apoE4 compared to apoE3.

The affinity constant values determined were compared with those achieved in our previous study for the interactions between apoE isoforms, apoE2 and apoE3, and another GAG chain of PGs – DS.[16] The affinity constant values were slightly higher for the apoE isoforms-C6S system (Table 1). Surprisingly, the heterogeneity of interactions of apoE isoforms with C6S differs from those with DS. For the apoE2-DS interaction, one site binding was observed while for apoE2-C6S two site binding was achieved. In addition, a difference was noticed for apoE3 isoform which indicates one site binding with C6S and two sites binding with DS. This kind of behavior can be explained by the structural differences within GAGs. Both of them inherit a long charged polysaccharide containing variable amount of iduronic acid.[26] The presence of iduronic acid in GAGs changes the properties of the polysaccharides generating a more flexible chain with increased binding potentials and allowing specific interactions with proteins.

Experimental

Materials

Phosphoric acid was obtained from Merck (Darmstadt, Germany), dimethyl sulfoxide, sodium hydroxide (1.0 M), and hydrochloric acid (0.1–1.0 M) were purchased from Oy FF-Chemicals (Yli Ii, Finland). C6S (M = 56 000 g mol^{-1}) was from Sigma (Darmstadt, Germany), and poly(2-vinylpyridine)-*block*-poly(ethylene oxide) ($M_{n,P2VP}$ = 3000 g mol^{-1}, $M_{n,PEO}$ = 10 000, M_w/M_n = 1.13) from Polymer Source inc. (124 Avro Street, Dorval (Montreal), QC, Canada). The peptide fragments of apoE were synthesized at the Meilahti Protein Chemistry Facility and analyzed at the Protein Chemistry Core Facility (Biomedicum, University of Helsinki, Finland) and reported earlier.[27]

Sample and buffer preparation

The ionic strengths of the BGE solutions (phosphate buffer at pH value 7.4) was 20 mM with pH adjusted to desired value with 1.0 M sodium hydroxide or 1.0 M hydrochloric acid. Before use, the BGE was filtered through 0.45 μm Millipore filters using a Millipore vacuum system. The pK_a value of 7.2 for phosphoric acid was used for calculations of ionic strength of the BGE.

The apoE isoforms and apoE-containing HDL$_2$ stock solutions were prepared in MilliQ water with a concentration ranging from 0.96 to 1.66 mg mL^{-1} and stored at −20 °C and +4 °C, respectively. Before injection stock solutions were diluted in running buffer to obtain 0.2 mg mL^{-1} as a final concentration. C6S stock solutions (0.1 mg mL^{-1}; 2.3 mg mL^{-1}) were prepared in MilliQ water and stored at +4 °C. Prior to

injection, solutions were diluted in running buffer to achieve samples with the concentrations ranging from 0.003 mg mL^{-1} to 1.0 mg mL^{-1}.

Instrumentation

The capillary electrophoretic experiments were carried out with a Hewlett-Packard Chemstation ^{3D}CE system (Agilent, Waldbronn, Germany) equipped with a diode-array detector (detection at 200 nm) and an air-cooling device for the capillary cassette. The temperature of the autosampler was controlled with an MGW Lauda K2 water-bath (Lauda-Königshofen, Germany), and all measurements were done at 25 °C. Uncoated fused-silica capillaries were from Optronis GmbH (Kehl, Germany). Dimensions were 50 μm i.d. and 375 μm o.d. The length of the capillary to the detector was 30.0 cm and the total length was 38.5 cm. A MeterLab PHM220 pH meter (Radiometer, Copenhagen, Denmark) was used to adjust the pH of the electrolyte solutions. Distilled water was purified with a Millipore water purification system (Millipore, Molsheim, France).

Calculations

The AEDs were iteratively calculated with the expectancy method by exploiting an in house made program.[18] In the AED calculations the energy was spanned with 400 grid points and 100 thousand iterations were used for all calculations except for apoE-containing HDL$_2$ where as many as one million iterations were used. The non-linear fitting was conducted using Levenberg–Marquardt algorithm implemented in SciPy. The non-linear model fit to the bi-Langmuir model has a constrained on the sum of the monolayer saturation capacity. This constrains and model fit were conducted also by exploiting the Levenberg–Marquardt algorithm.

All calculations were conducted by Python 3.4.2 using the lmfit 0.8.2, SciPy 0.15.0, NumPy 1.9.1 and visualized using Matplotlib 1.4.2 libraries. Because all these libraries and Python are open source, they are readily available for most operational systems.

Capillary electrophoresis studies

Coating procedure. To diminish strong and unfavorable adsorption of the positively charged biomolecules on the negatively charged fused-silica capillary, the capillary wall was coated with quaternized double-hydrophilic poly(N-methyl-2-vinyl pyridinium iodide-block-ethylene oxide) (P2QVP-b-PEO) diblock copolymer.[21] Briefly, uncoated fused-silica capillary (L_{tot} 38.5 cm, L_{det} 30 cm) was firstly pretreated by flushing it 20 min with 1 M HCl, 10 min with 0.1 M HCl, 25 min with Milli-Q water, 5 min with a BGE solution at a pressure of 940 mbar. After pretreatment, the capillary was rinsed with P2QVP-b-PEO for 40 min and then left to stand for 30 min to finalize the coating. To remove the unreacted copolymer solution, the capillary was treated for 60 min with BGE solution (phosphate buffer, pH 7.4, I 20 mM) at a pressure of 940 mbar. Next, the EOF was determined by exploiting the Williams and Vigh method.[22]

Partial filling procedure. The partial filling procedure has been described in slightly different way in our previous studies.[13–16] Briefly, negatively charged analytes were hydrodynamically introduced to the coated capillary. Firstly, either isoform of apoE or apoE-containing HDL$_2$ was introduced for 2 s at 50 mbar and then C6S for 3 s at 50 mbar in the concentration ranging from 0.003 mg mL^{-1} to 1.0 mg mL^{-1}. Next, a voltage of −25 kV was applied, and both analytes started to move towards to anode at the detector end. Highly negatively charged C6S reached either negatively charged isoform of apoE or apoE-containing HDL$_2$ and the resulting complex formed moved to the detector. The migration time of apoE-C6S or apoE-containing HDL$_2$-C6S decreased as the number of negative charges in C6S increased. The detection was performed at wavelength 200 nm. Before each run, the capillary was rinsed for 2 min with the BGE solution to equilibrate the capillary. In addition, the EOF mobility was controlled between runs to guarantee the stability of the coating.

Determination of affinity constants

To determine the affinity constants for apoE isoforms or apoE-containing HDL$_2$-C6S complexes, the AED calculations were introduced. First, the fractions of apoE isoform or apoE-containing HDL$_2$ bound to C6S were established as a function of C6S concentrations. Constant concentration and volume of apoE isoform or apoE-containing HDL$_2$ was injected first followed by injection of C6S with increasing concentrations. After the voltage was applied, C6S with higher mobility due to a high number of negative charges reached apoE isoform or apoE-containing HDL$_2$ and interacted with it. The binding of apoE isoform or apoE-containing HDL$_2$ with receptor (C6S) increased the number of charges and its average mobility that can be described based on the following equation:[28]

$$\mu^A = \Theta_f \mu_f + \Theta_b \mu_b \qquad (1)$$

where, Θ_f and Θ_b are the free and bound fraction of apoE isoform or apoE-containing HDL$_2$, respectively, and μ_f and μ_b are the mobilities of free and bound apoE isoform or apoE-containing HDL$_2$ to C6S, and μ^A is the average mobility of the complex. Because $\Theta_f + \Theta_b = 1$, the equation for adsorbed fraction can be described as:

$$\Theta_b = \frac{\mu^A - \mu_f}{\mu_b - \mu_f} \qquad (2)$$

The mobilities of the adsorbed and free fractions were investigated with exponential and linear fitting, respectively. At the lower end of the concentration range, electrophoretic mobility was linearly decreased towards the minimum value, where apoE isoform or apoE-containing HDL$_2$ was in free form. At the high concentration end, where apoE isoform or apoE-containing HDL$_2$ was totally bound to C6S, electrophoretic mobility reached the maximum value.

Adsorption energy distribution calculations

Adsorption isotherms describe the relation between adsorbed and free concentrations of analyte at a constant and specific temperature.[29] The most often used adsorption model describing homogeneous interactions is the Langmuir model and can be expressed as:

$$\Theta_b = \frac{KC}{1 + KC} \qquad (3)$$

where K is the association equilibrium constant. Many times the interactions of analytes to a surface are heterogenic and the other adsorption models have to be used. The bi-Langmuir model describes two independent adsorption sites with different adsorption energy (equilibrium constant):

$$\Theta_b = \Theta_{max,1} \frac{K_1 C}{1 + K_1 C} + \Theta_{max,2} \frac{K_2 C}{1 + K_2 C} \qquad (4)$$

where $\Theta_{max,i}$ and K_i are the monolayer saturation capacity and the association equilibrium constant for the ith adsorption site, respectively. In this model the sum of $\Theta_{max,1}$ and $\Theta_{max,2}$ is equal to 1 and this constrain is used in the non-linear model fitting to the bi-Langmuir model. The degree of heterogeneity in the energy of interactions is evaluated by AED calculations by expanding eqn (4) to a continuous distribution of independent adsorption sites over certain adsorption energy range. In this way the adsorption isotherm becomes an integral equation and can be expressed as:

$$\Theta_b = \int_{K_{min}}^{K_{max}} f(\ln K) \Theta(C, K) \, d \ln K \qquad (5)$$

where $\Theta(C,K)$ is the local adsorption isotherm model and $f(\ln K)$ is the AED. K_{min} and K_{max} are calculated from $0.1/C_{max}$ and $10/C_{min}$, respectively, where C_{max} is the maximum concentration used in the adsorption isotherm determination and C_{min} is the lowest concentration. The AED is solved iteratively using the expectation maximization method.[30]

Conclusions

Integration of adsorption energy distribution calculations with partial filling affinity electrophoresis was successfully exploited to get insight into the strength of the binding processes between major apoE isoforms (apoE2, apoE3 and apoE4) and main GAG chain of PGs – C6S. The stable P2QVP-*b*-PEO coating throughout the whole study eliminated cationic adsorption problems, so that even small differences in the interactions could be distinguished. In addition, AED analysis was crucial in the elucidation of the heterogeneity of the interactions and clarified the order of binding strength between apoE isoforms and C6S. Although Scatchard plots were not always able to distinguish a heterogeneous and homogeneous adsorption model due to experimental noise, AED calculations delivered good data in such cases. The binding processes for apoE2 isoform-C6S and apoE4 isoform-C6S were bimodal,

while surprisingly only one site binding process was characterized for apoE3 isoform and apoE-containing HDL$_2$. The developed AED-PF-ACE method provided an excellent platform for the elucidation of changes in the interactions even due to only one amino acid mutation. Namely apoE isoforms differ in structure at amino acids residues 112 and 158 affecting their properties and relation to diseases. The results exposed that the utilization of AED calculations in the capillary electrophoretic biomolecular interactions studies offer a promising reliable and a powerful tool to establish the heterogeneity of biological processes.

Acknowledgements

Notes and references

1 M. S. Brown, P. T. Kovanen and J. L. Goldstein, *Science*, 1981, **212**, 628–635.

2 T. Hevonoja, M. O. Pentikäinen, M. T. Hyvönen, P. T. Kovanen and M. Ala-Korpela, *Biochim. Biophys. Acta*, 2000, **1488**, 189–210.

3 M. H. Wang and M. R. Briggs, *Chem. Rev.*, 2004, **104**, 119–137.

4 M. S. Brown and J. L. Goldstein, *N. Engl. J. Med.*, 1981, **305**, 515–517.

5 K. J. Williams and I. Tabas, *Atheriocler., Thromb., Vasc. Biol.*, 2005, **25**, 1536–1540.

6 K. Skålen, M. Gustafsson, E. K. Rydberg, M. Hulten, O. Wiklund, T. L. Innerarity and J. Boren, *Nature*, 2002, **417**, 750–754.

7 B. Radhakrishnamurthy, R. S. Srinivasan, P. Vijayagopal and G. S. Brenson, *Eur. Heart J.*, 1990, **11**, 148–157.

8 R. L. Jackson, S. J. Busch and A. D. Cardin, *Physiol. Rev.*, 1991, **71**, 481–539.

9 K. D. O'Brien, K. Olin, C. E. Alpers, W. Chiu, M. Ferguson, K. Hudkins, T. N. Wight and A. Chait, *Circulation*, 1998, **98**, 519–527.

10 J. M. Trowbridge and R. L. Gallo, *Glycobiology*, 2002, **12**, 117–125.

11 S. C. Rall, K. H. Weisgraber and R. W. Mahley, *J. Biol. Chem.*, 1982, **257**, 4174–4178.

12 J. Dong, A. Peters-Libeu, K. H. Weisgraber, B. W. Segelke, B. Rupp, I. Capila, M. J. Hernaiz, L. A. LeBrun and R. J. Linhardt, *Biochemistry*, 2001, **40**, 2826–2834.

13 A. J. Wang, K. Vainikka, J. Witos, L. D'Ulivo, G. Cilpa, P. T. Kovanen, K. Öörni, M. Jauhiainen and M.-L. Riekkola, *Anal. Biochem.*, 2010, **399**, 93–101.

14 K. Lipponen, P. W. Stege, G. Cilpa, J. Samuelsson, T. Fornstedt and M.-L. Riekkola, *Anal. Chem.*, 2011, **83**, 6040–6046.

15 G. Cilpa-Karhu, K. Lipponen, J. Samuelsson, K. Öörni, T. Fornstedt and M.-L. Riekkola, *Anal. Biochem.*, 2012, **443**, 39–147.

16 K. Lipponen, S. Tähkä, J. Samuelsson, M. Jauhiainen, J. Metso, G. Cilpa-Karhu, T. Fornstedt, M. Kostiainen and M.-L. Riekkola, *Anal. Bioanal. Chem*, 2014, **406**, 4137–4146.

17 V. A. Hernandez, J. Samuelsson, P. Forssen and T. Fornstedt, *J. Chromatogr., A*, 2013, **1317**, 22–31.

18 J. Samuelsson, A. Franz, B. J. Stanley and T. Fornstedt, *J. Chromatogr., A*, 2007, **1163**, 177–189.

19 J. Samuelsson, R. Arnell and T. Fornstedt, *J. Sep. Sci.*, 2009, **32**, 1491–1506.

20 X. Zhang, J. Samuelsson, J.-C. Janson, C. Wang, Z. Su, M. Gu and T. Fornstedt, *J. Chromatogr. A*, 2010, **1217**, 1916–1925.

21 K. Lipponen, S. Tähkä, M. Kostiainen and M.-L. Riekkola, *Electrophoresis*, 2014, **35**, 1106–1113.

22 B. A. Williams and C. Vigh, *Anal. Chem.*, 1996, **68**, 1174–1180.

23 G. Götmar, J. Samuelsson, A. Karlsson and T. Fornstedt, *J. Chromatogr. A*, 2007, **1156**, 3–13.

24 K. H. Weisgraber, *Adv. Protein Chem.*, 1994, **45**, 249–302.

25 R. W. Mahley and S. C. Rall Jr., *Annu. Rev. Genomics Hum. Genet.*, 2000, **1**, 507–537.

26 M. A. Thelin, B. Bartolini, J. Axelsson, R. Gustafsson, E. Tykesson, E. Pera, A. Oldberg, M. Maccarana and A. Malmstrom, *FEBS J.*, 2013, **230**, 2431–2446.

27 L. D'Ulivo, J. Witos, K. Öörni, P. T. Kovanen and M.-L. Riekkola, *Electrophoresis*, 2009, **30**, 3838–3845.

28 N. Fang, H. Zhang, J. Li, H.-W. Li and E. S. Yeung, *Anal. Chem.*, 2007, **79**, 6047–6054.

29 G. Guiochon, A. Felinger, D. G. Shirazi and A. Katti, *Fundamentals of Preparative and Nonlinear Chromatography*, Elsevier Academic, San Diego, 2nd edn., 2006.

30 B. J. Stanley, S. E. Bialkowski and D. B. Marshall, *Anal. Chem.*, 1993, **85**, 259–267.